Nuclear-Reaction Studies in the Nickel Isotopes: The $Ni^{58}(p,p')Ni^{58}$ and $Ni^{58}(d,p)Ni^{59}$ Reactions*

E. R. Cosman, C. H. Paris,† A. Sperduto, and H. A. Enge

Laboratory for Nuclear Science and Department of Physics, Massachusetts Institute of Technology, Cambridge, Massachusetts

(Received 16 September 1965)

The reactions $Ni^{58}(p,p')Ni^{58}$ and $Ni^{58}(d,p)Ni^{59}$ have been studied at a bombarding energy of 7.0 MeV using the MIT–ONR Van de Graaff generator and both the single-gap and multiple-gap broad-range spectrographs. With an energy resolution of better than 10 keV, fourteen levels in Ni^{58} were observed up to 4.2-MeV excitation; and in Ni^{59}, 173 levels were observed up to an excitation energy of 7.5 MeV. Q values and positions of energy levels for both reactions have been measured with accuracies between 5 and 10 keV using the single-gap spectrograph. In the $Ni^{58}(d,p)Ni^{59}$ investigation, simultaneous proton spectra were obtained at 24 reaction angles with the multiple-gap spectrograph. The angular distribution of the proton groups showing stripping characteristics were analyzed by use of the distorted-wave Born approximation. Absolute differential cross sections for all levels have been measured, and the values of l_n, the orbital angular momentum of the transferred neutron, and the strength functions $(2J+1)S_{l_n,j}$ for the stripping levels have been obtained. A sum-rule analysis is made, and the results are compared with shell-model predictions.

I. INTRODUCTION

CHARGED-particle studies of the energy levels in the nickel isotopes have been undertaken in this laboratory over the past several years. Some results have been reported in the Laboratory for Nuclear Science Progress Reports and in the Bulletin of the American Physical Society.[1] In this paper, we present our complete data from the $Ni^{58}(d,p)Ni^{59}$ and the $Ni^{58}(p,p')Ni^{58}$ reactions. Subsequent publications will discuss the (p,p'), (d,p), and (d,d') reactions on the other stable isotopes of nickel.

The simple shell model describes low-lying states of the nickel isotopes as having cores of 28 neutrons and 28 protons closing the $1f_{7/2}$ shell, with the surplus neutrons occupying the $2p_{3/2}$, $1f_{5/2}$, and $2p_{1/2}$ subshells. With the introduction of residual interactions, keeping the core inert, theory can qualitatively account for the collective vibrations seen in the even Ni isotopes, as well as for observed configuration mixing of higher orbitals in the Ni ground states.[2,3] Present models, however, are still approximate and thus probably over-simplify the picture of nuclear structure in this region. Adequate testing of the theories requires more detailed experimental data and, in the case of nuclear reactions, a closer examination of the methods by which spectroscopic information is extracted.

In recent years, a large amount of data from stripping[4,5] and pickup[6-8] reactions in Ni^{58} have appeared in the literature. The higher energy resolution and use of isotopically pure targets in the present work have made it possible to identify many new levels in Ni^{59}. These refinements are particularly important for distinguishing levels above 2.5-MeV excitation where the level density is rapidly increasing to thirty levels per MeV and more. Below 7.5-MeV excitation in Ni^{59} we have seen twice as many levels as have been previously reported by other investigators.

In the previous preliminary reports from this laboratory,[1] the Butler plane-wave theory was used to analyze the nickel (d,p) data. It is well known that the cross sections predicted from such a theory are too large by about one order of magnitude. Calculations based on distorted-wave Born approximation (DWBA) have recently met with greater success, both in fitting the experimental angular distributions and in predicting the absolute cross sections.

Consequently, it was felt that a reanalysis of our data, using a DWBA calculation would be desirable at this time, not only to deduce a consistent set of spectroscopic information for the nickel isotopes, but also to permit comparisons with other stripping analyses using

---

[1] C. H. Paris, MIT-LNS Progress Reports, 1956-59, inclusive (unpublished); W. W. Buechner, Bull. Am. Phys. Soc. 2, 61 (1957), and 3, 38 (1958); M. Mazari, W. W. Buechner, and R. de Figueiredo, Phys. Rev. 108, 373 (1957); R. A. Fisher and H. A. Enge, Bull. Am. Phys. Soc. 4, 287 (1959); H. A. Enge et al., MIT-LNS Progress Reports 1958, 1959, 1961 (unpublished); H. A. Enge, W. W. Buechner, J. R. Erskine, J. A. Taylor, H. J. Hennecke, and A. Sperduto, Bull. Am. Phys. Soc. 6, 342 (1961); K. Moriyasu, J. L. Adams, and H. A. Enge, MIT-LNS Progress Report, 1963 (unpublished).

[2] L. S. Kisslinger and R. A. Sorenson, Kgl. Danske Videnskab. Selskab, Mat. Fys. Medd. 32, No. 9 (1960), and Rev. Mod. Phys. 35, 853 (1963).

[3] R. Arvieu, E. Salusti, and M. Veneroni, Phys. Letters 8, 334 (1964) and K. Sorensen, Nucl. Phys. 25, 674 (1961).

[4] R. H. Fulmer, A. L. McCarthy, B. L. Cohen, and R. Middleton, Phys. Rev. 133, 955 (1964).

[5] A. W. Dalton, G. Parry, H. D. Scott, and S. Swierszczewski, Proc. Phys. Soc. (London) 77, 682 (1961) and J. P. Schiffer, L. L. Lee, Jr., and B. Zeidman, Phys. Rev. 115, 427 (1959).

[6] J. C. Legg and E. Rost. Phys. Rev. 134, 752 (1964); R. Sherr, E. Rost, and M. E. Rickey, Phys. Rev. Letters 12, 420 (1964); and R. Sherr, B. F. Bayman, E. Rost, M. E. Rickey, and C. G. Hoot, Phys. Rev. 139, B1272 (1965).

[7] G. Bassani, N. Hintz, and C. D. Kavaloski, Phys. Rev. 136, 1006 (1964).

[8] M. H. Macfarlane, B. J. Raz, J. L. Yntema, and B. Zeidman, Phys. Rev. 127, 204 (1962); and R. H. Fulmer and W. W. Daehnick, ibid. 139, B579 (1965).

similar measurement techniques in this laboratory for nuclei in the $f_{7/2}$ shell.

The reaction data discussed in previous preliminary reports have been augmented more recently with additional experiments on the angular distributions of elastic and inelastic scattering of deuterons from some of the nickel isotopes. The elastic-scattering data have been used here to deduce parameters for the optical-model potentials needed for the DWBA reaction calculations. The computer code JULIE was used for these calculations, which were performed on an IBM 7094 at the MIT Computation Center.

II. EXPERIMENTAL METHODS

Deuteron and proton beams were accelerated to 7.0 MeV by the MIT-ONR electrostatic generator, deflected 90 deg in an analyzing magnet, and allowed to impinge upon thin-film nickel targets. The (p,p') experiment consisted of one set of exposures carried out on the single-gap broad-range spectrograph[9] at reaction angles $\theta_{lab} = 20$, 50, and 130 deg. Two sets of (d,p) exposures were made, one early set (at $\theta_{lab} = 20$, 50, and 130 deg) utilizing the single-gap instrument and one more recent set utilizing the multiple-gap spectrograph.[10] This instrument is similar to the single-gap magnetic spectrograph, except that it has 25 gaps instead of one and thus permits the simultaneous recording of broad-range spectra at 25 angles. The gaps are located every 7.5 deg from 0 to 172.5 deg, with respect to the incident beam. However, the 0-deg gap cannot normally be utilized, and there are two 90-deg gaps, one on each side of the beam. The photographic plates used to record proton tracks in the (d,p) exposure were covered with aluminum foils of about 0.003-in. thickness. This was sufficient to stop deuterons from the target before they reached the emulsions, and scanning difficulties were thereby reduced. In the (p,p') and (d,p) reactions, the targets were ex-

posed to the beam for 1000 and 3000 μC, respectively. After exposure, the photographic plates that were placed along the focal plane of the magnetic spectrograph were developed and scanned under a microscope.

Targets for the (p,p') exposure were prepared by vacuum evaporation of natural nickel metal onto Formvar backings supported by a 1-in.-diam circular frame. Enriched Ni^{58} obtained from Oak Ridge National Laboratory was used in the target for the (d,p) experiments. The isotopic analysis of this target was Ni^{58}, 99.6%; Ni^{60}, 0.3%; Ni^{61}, none; Ni^{62}, 0.1%; and Ni^{64}, none. Proton peaks from reactions on contaminants, such as S^{32}, O^{16}, and C^{12}, present in the target and backing were distinguished from the nickel spectra by means of their different energy shift versus angle.

During the multiple-gap exposure, the target was rotated at 200 rpm about an axis normal to the target plane. The beam hit the target off center so that a ring was exposed over a total area of about 100 times the beam cross section. This helped in heat dissipation, and the surface contamination that builds up at the beam spot was smeared out over a larger area and consequently formed a thinner layer than on a nonrotating target. The target thickness, which is important for establishing absolute cross sections, was first estimated by measurements[11] with an alpha-particle thickness gauge, and was later measured accurately by Rutherford elastic scattering of deuterons at 3.0 MeV. The thickness in the beam direction was 17.8 $\mu g/cm^2$.

Absolute Q values for the $Ni^{58}(d,p)Ni^{59}$ reaction were taken from the earlier exposures on the single-gap spectrograph, since this instrument is somewhat more accurate than the multiple-gap spectrograph. The calibration of both instruments is based on the use of alpha particles from Po^{210}, and the energy of these alpha particles was originally taken to be 5.299 ± 0.005 MeV.[12] Earlier preliminary reports[1] on the energy levels of Ni^{58}
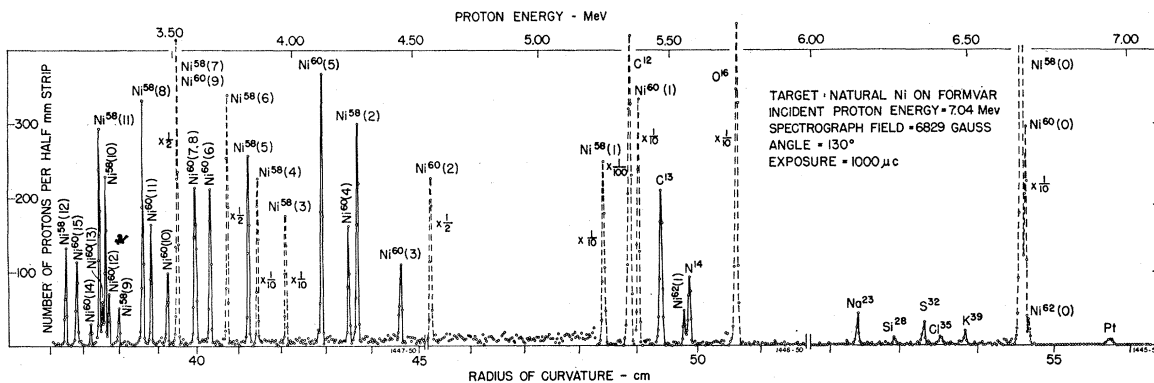
FIG. 1. Spectrum of protons emitted from a nickel-on-Formvar target bombarded with 7.04-MeV protons. Observation angle $\theta_{lab} = 130°$, single-gap spectrograph. Proton groups identified by their kinematic shift as being levels in Ni^{58} are labeled with the numbers used to identify these states in Table I. Prominent groups from contaminants and other nickel isotopes present in the target are also identified.

[9] C. P. Browne and W. W. Buechner, Rev. Sci. Instr. **27**, 899 (1956).
[10] H. A. Enge and W. W. Buechner, Rev. Sci. Instr. **34**, 155 (1963).
[11] H. A. Enge, M. A. Wahlig, and I. Aanderaa, Rev. Sci. Instr. **28**, 145 (1957).
[12] E. N. Strait, D. M. Van Patter, W. W. Buechner, and A. Sperduto, Phys. Rev. **81**, 747 (1951).
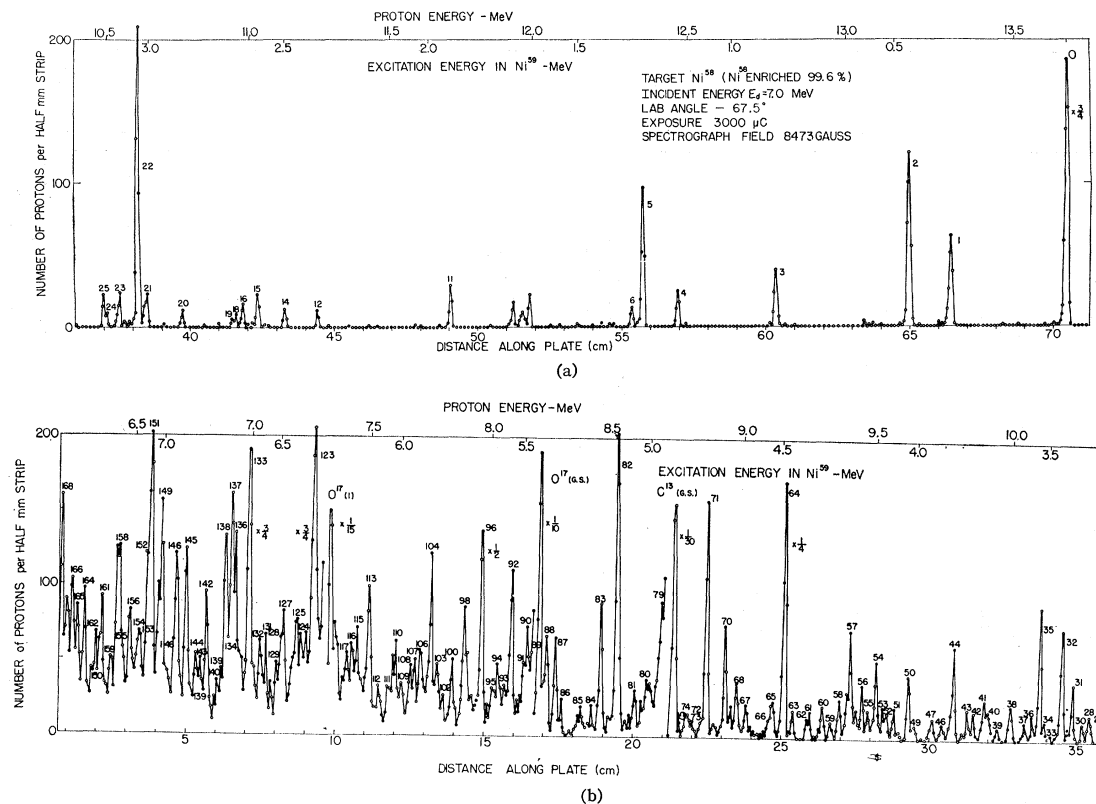
FIG. 2. Measured proton spectrum from the Ni⁵⁸(d,p)Ni⁵⁹ reaction at a deuteron bombarding energy of 7.0 MeV and laboratory reaction angle of 67.5°, multiple-gap spectrograph. The proton groups are labeled with the numbers used to identify the corresponding states in Ni⁵⁹ listed in Table II.

and Ni⁵⁹ were thus based on that standard. The Q values and excitation energies reported in the present paper have been corrected by approximately 0.1% to reflect the adoption in our laboratory of a new more precise energy value 5.3042±0.0012 MeV for this standard.[13] The MIT 7094 computer was used to calculate Q as a function of distance along the photographic plate with the known incident energy, spectrograph field, reaction angle, and spectrograph calibration constants as input parameters.

III. EXPERIMENTAL RESULTS

Typical spectra from the (p,p′) and (d,p) reactions are shown in Figs. 1 and 2, respectively. In these experiments, fourteen levels in Ni⁵⁸ below 4.2-MeV excitation and 173 levels in Ni⁵⁹ below 7.54-MeV excitation were resolved. In the experiment with the multiple-gap spectrograph, two levels in Ni⁵⁹ were detected that had not been seen in the earlier single-gap (d,p) experiment. The energies of the excited levels in Ni⁵⁸ are listed in Table I. No further discussion will be made of the Ni⁵⁸ spectrum except in Sec. V where a brief comparison is

[13] W. W. Buechner, *Proceedings of the International Conference on Nuclidic Masses*, edited by H. E. Duckworth (University of Toronto Press, Hamilton, Ontario, 1960), p. 263.

made with levels in Ni⁵⁹. The energy levels and corresponding Q values for the Ni⁵⁸(d,p)Ni⁵⁹ reaction are given in columns 2 and 3 of Table II. The quoted results are arithmetic averages of energies determined at a minimum of two reaction angles. The uncertainties in these excitation energies were estimated as ±5 keV, standard error, for the lowest states and ±10 keV for the highest excited states. The ground-state Q value for the Ni⁵⁸(d,p)Ni⁵⁹ reaction was found to be 6.785±0.005 MeV.

TABLE I. N⁵⁸ levels up to 4.1 MeV.

Level number	Excitation energy (MeV)
1	1.452±0.005
2	2.458±0.005
3	2.772±0.005
4	2.899±0.005
5	2.939±0.005
6	3.035±0.005
7	3.260±0.005
8	3.418±0.005
9	3.528±0.005
10	3.592±0.005
11	3.630±0.005
12	3.774±0.005
13	3.898±0.005
14	4.106±0.005

TABLE II. Ni^{59} levels up to 7.5 MeV.

Level No.	E_x (MeV)	Q (MeV)	θ_{max} (deg)	$(d\sigma/d\Omega)_{max}$ (mb/sr)	l_n	$(2J+1)S$	E_x (MeV)	l_n	$(2J+1)S$
			Present work				Fulmer et al. (Ref. 4)		
0	0	6.785	17	4.60	1	2.74	0	1	2.77
1	0.341	6.444	37	0.754	3	4.05	0.340	3	5.19
2	0.466	6.319	18	2.20	1	1.26	0.471	1	1.24
3	0.880	5.905	18	0.64	1	0.324	0.887	1	0.311
4	1.193	5.593		0.119	n.s.[a]				
5	1.307	5.478	18	1.11	1	0.519	1.318	1	0.561
6	1.345	5.440	15	0.101	n.s.		1.348		
7	1.685	5.100	45	0.145	3	0.737	1.696	(3)	0.605
8	1.737	5.048		0.111	n.s.		1.748	(1)	0.031
9	1.748	5.037		(0.020)	n.s.				
10	1.776	5.009		(0.040)	n.s.				
11	1.953	4.832		0.138	n.s.		1.967		
12	2.418	4.367	31	0.160	2	0.104	2.422	(1)	0.025
13	2.428	4.357		(0.021)	n.s.				
14	2.533	4.252		0.041	n.s.				
15	2.633	4.152	23	0.190	(1)	0.067	2.640	3	0.307
16	2.683	4.102		0.065	n.s.		2.698		
17	2.692	4.093		<0.020	n.s.				
18	2.705	4.080		0.020	n.s.				
19	2.718	4.067		(0.021)	n.s.				
20	2.901	3.884	15	0.072	(1)	0.025	2.910	1	0.006
21	3.035	3.750	15	0.200	(1)	0.070	3.045	1	0.032
22	3.060	3.725	46	0.900	4	10.600	3.071	4	7.50
23	3.132	3.653		0.063	n.s.		3.151		
24	3.186	3.599 }	23	0.186	1	0.065	3.203	1	0.030
25	3.196	3.589 }							
26	3.310	3.475 }		0.074	n.s.				
27	3.324	3.461 }			n.s.				
28	3.356	3.429 }	(15–30)	0.143	(1)	0.049	3.384	2	0.011
29	3.372	3.413 }							
30	3.386	3.399		0.035	n.s.				
31	3.424	3.361	0	0.50	0	0.038	3.421	0	0.046
32	3.461	3.324	(15–23)	0.450	1	0.143	3.468	1	0.154
33	(3.515)	(3.270)		0.034	n.s.				
34	(3.531)	(3.254)		0.052	n.s.				
35	3.544	3.241	22	0.375	1	0.117	3.559	2	0.197
36	3.573	3.212	22	0.086	1	0.025			
37	3.600	3.185			n.s.				
38	3.648	3.137		0.075	n.s.		3.661	2	0.031
39	3.696	3.089	31	0.075	2	0.040	3.711	2	0.017
40	3.728	3.057 }	(33)	0.145	n.s.				
41	3.745	3.040 }			n.s.				
42	3.791	2.994		0.036	n.s.				
43	3.812	2.973		0.043	n.s.				
44	3.866	2.919	23	0.368	1	0.105	3.874	1	0.101
45	3.898	2.887		<0.030	n.s.				
46	3.910	2.875		0.062	n.s.		3.920		
47	3.944	2.841		0.049	n.s.				
48	4.005	2.750		<0.030	n.s.				
49	4.015	2.770		0.048	n.s.				
50	4.036	2.749	22	0.198	1	0.053	4.031	1	0.052
51	4.087	2.698	(37)	0.085	(2)	(0.047)	4.054	(0)	0.002
52	4.120	2.665		(0.050)	n.s.				
53	4.133	2.652		(0.055)	n.s.				
54	4.154	2.631	(20)	0.273	1	0.027	4.145	1	0.054
55	4.177	2.608		(0.050)	n.s.				
56	4.213	2.572	(52)	0.099	(3)	0.398	4.210	2	0.064
57	4.264	2.520	20	0.429	1	0.110	4.256	(1)	0.118
58	4.293	2.492		0.100	n.s.		4.294		
59	4.328	2.457	(30)	0.104	n.s.				
60	4.356	2.429	(33)	0.145	2	0.086			
61	4.407	2.378 }	0	0.200	(0)	0.013			
62	4.419	2.366 }							
63	4.470	2.315	0	(0.150)	(0)	0.008	4.469	4	0.408
64	4.506	2.279	33–37	2.80	2	1.44	4.505	2	1.44
65	4.543	2.242		<0.050	n.s.				
66	4.557	2.228		<0.050	n.s.				
67	4.646	2.139		0.110	n.s.		4.611	2	0.014
68	4.650	2.105	(42)	0.140	n.s.		4.652		
69	4.709	2.076	(15–30)	0.090	(1)	0.026	4.691	4	0.716
70	4.728	2.057	22	0.268	1	0.057	4.734	1	0.078

TABLE II (continued)

Level No.	E_x (MeV)	Q (MeV)	Present work θ_{max} (deg)	$(d\sigma/d\Omega)_{max}$ (mb/sr)	l_n	$(2J+1)S$	Fulmer et al. (Ref. 4) E_x (MeV)	l_n	$(2J+1)S$
71	4.799	1.986	30	0.509	2	0.212	4.808	2	0.257
72	4.822	1.963		0.057	n.s.				
73	4.856	1.929		<0.060	n.s.				
74	4.869	1.916		<0.060	n.s.				
75	4.887	1.898		<0.040	n.s.		4.883	1	0.005
76	4.920	1.865		<0.060	n.s.		4.920		
77	4.939	1.846		<0.070	n.s.				
78	4.960	1.825	(15–30)	(0.140)	(1)	0.032	4.974	1	0.048
79	4.980	1.805	15–30	0.284	1	0.073	4.984	1	0.046
80	5.036	1.749	23	0.206	1	0.051	5.037	1	0.009
81	5.080	1.705	25–30	0.198	1	0.043			
82	5.149	1.636	0	4.30	0	0.175	5.159	0	0.15
83	5.213	1.572	30	0.396	2	0.165	5.219	2	0.140
84	5.258	1.527		0.050	n.s.				
85	5.292	1.493	15–25	0.100	1	0.028			
86	5.372	1.412		0.060	n.s.				
87	5.395	1.390	30	0.240	2	0.093	5.389	2	0.099
88	5.429	1.356	(63)	0.167	n.s.		5.425	4	0.816
89	5.458	1.327	37	0.685	2	0.318	5.461	2	0.310
90	5.508	1.277⎫	22	(0.468)	(1)	0.061	5.505	1	0.041
91	5.528	1.257⎭					5.534		
92	5.569	1.216	0	1.50	0	0.092	5.570	0	0.126
93	5.608	1.177⎫							
94	5.629	1.156⎬	(45)	0.315			5.620	1	0.040
95	5.648	1.137⎭							
96	5.692	1.093	0	5.50	0	0.256	5.692	0	0.268
97	5.747	1.038		(0.060)	n.s.				
98	5.762	1.023	22	0.460	1	0.095	5.774	1	0.061
99	5.783	1.002		(0.060)	n.s.				
100	5.805	0.980	30	0.213	2	0.076	5.807	(2)	0.029
101	5.821	0.964		<0.080	n.s.				
102	5.844	0.941	30	(0.080)	2	0.027			
103	5.872	0.913		(0.150)	n.s.				
104	5.894	0.891	(30)	(0.420)	(2)	0.144	5.890	2	0.164
105	5.924	0.861	(15–30)	(0.055)					
106	5.946	0.839					5.940		
107	5.967	0.818	30–60	0.480	2	0.158			
108	5.988	0.797					5.978	1	0.047
109	6.013	0.772		<0.070	n.s.				
110	6.034	0.751	22	0.300	(1)	0.061	6.049		
111	6.071	0.714		<0.100	n.s.				
112	6.114	0.671	22	0.260	(1)	0.053	6.116	2	0.025
113	6.149	0.636	22	0.420	1	0.082	6.150	(1)	0.050
114	6.189	0.596		(0.050)	n.s.				
115	6.206	0.579	30	(0.240)	2	0.072			
116	6.225	0.560	15–20	0.210	1	0.042	6.220	2	0.112
117	6.245	0.540	20–30	0.163	(1)	0.031	6.249	2	0.052
118	6.269	0.516		<0.050	n.s.				
119	6.284	0.501	15	0.180	n.s.				
120	6.305	0.480	30	0.630	2	0.203	6.306	2	0.292
121	6.339	0.446⎫	23	0.155	1	0.029	6.341	(2)	0.041
122	6.354	0.431⎭							
123	6.380	0.405	0	2.4	0	0.173	6.380	0	0.175
124	6.434	0.351⎫							
125	6.454	0.331⎬	15	0.374	(1)	0.035	6.450	2	0.056
126	6.481	0.304⎭							
127	6.507	0.278⎫	28	0.510	1	0.106	6.513	2	0.083
128	6.521	0.264⎭							
129	6.535	0.250		<0.060	n.s.		6.544	(2)	0.018
130	6.567	0.218⎫	≤22	0.25			6.597	0	0.022
131	6.583	0.202⎭							
132	6.605	0.180	≤30	0.20			6.618	2	0.040
133	6.648	0.137	33	0.715	2	0.226	6.657	2	0.270
134	6.679	0.106			n.s.				
135	6.690	0.095	0	(0.25)	0	0.016			
136	6.709	0.076	37	0.457	2	0.152			
137	6.726	0.059	37	0.378	2	0.127	6.716	2	0.198
138	6.749	0.036	37	0.515	2	0.171	6.741	2	0.182
139	6.771	0.014		<0.100	n.s.				
140	6.788	−0.003		<0.100	n.s.				
141	6.806	−0.021		<0.100	n.s.				

TABLE II *(Continued)*

Level No.	E_x (MeV)	Q (MeV)	θ_{max} (deg)	$(d\sigma/d\Omega)_{max}$ (mb/sr)	l_n	$(2J+1)S$	E_x (MeV)	l_n	$(2J+1)S$
			Present work				Fulmer *et al.* (Ref. 4)		
142	6.834	−0.048	20–30	0.273	2	0.081	6.843	2	0.072
143	6.859	−0.074 }	22	0.310	1	0.042			
144	6.880	−0.095 }							
145	6.919	−0.134	0	0.500	0	0.039	6.931	0	0.064
146	6.955	−0.170	0	0.95	0	0.056	6.967	0	0.07
147	6.974	−0.189		0.100	n.s.				
148	6.994	−0.210		0.080	n.s.				
149	7.023	−0.238 }	(30)	(0.65)	(2)	0.195	7.021	2	0.159
150	7.042	−0.257 }							
151	7.073	−0.288	(30)	0.83	2	0.260	7.080	2	0.047
152	7.092	−0.307		<0.100	n.s.				
153	7.111	−0.327 }							
154	7.124	−0.339 }	47	0.325	n.s.		7.129	2	0.056
155	7.141	−0.356 }							
156	7.160	−0.376	0	0.25	0	0.016	7.170		
157	7.187	−0.402		<0.100	n.s.				
158	7.204	−0.419	0	(0.70)	0	0.078	7.199		
159	7.237	−0.452	(37)	0.31	2	0.082	7.245	2	0.093
160	7.263	−0.478							
161	7.282	−0.497					7.287	2	0.090
162	7.304	−0.519							
163	7.324	−0.539							
164	7.353	−0.569							
165	7.384	−0.599					7.362	2	0.076
166	7.408	−0.623					7.394	2	0.060
167	7.434	−0.649					7.417	2	0.103
168	7.455	−0.671					7.448	2	0.155
169	7.478	−0.693							
170	7.491	−0.706							
171	7.504	−0.719							
172	7.521	−0.737							
173	7.539	−0.754					7.540	0	0.055

a Nonstripping.

Figures 3 and 4 show angular distributions of some of the more typical and prominent proton groups from the $Ni^{58}(d,p)Ni^{59}$ reaction. The points are the experimental cross sections plotted against reaction angle in the center-of-mass system, and the solid lines are the DWBA predictions. The position of the first forward-angle maximum θ_{max} in the stripping curves is critically dependent on l_n, the orbital angular momentum of the captured neutron. The positions of these maxima vary very little for positive Q values in this mass region and are characteristically 20, 30, and 40 deg for $l_n=1$, 2, and 3, respectively, at this bombarding energy. The $l_n=0$ curves have a sharp rise for decreasing angle from about 30 deg down to zero deg. Included in Table II are the values of $(d\sigma/d\Omega)_{max}$, θ_{max}, and for the levels displaying stripping angular distributions, the l_n values assigned, and the strength function $(2J+1)S_{l_n,j}$. When the angular distributions show a nonstripping pattern, the corresponding levels are designated "n.s." in Table II. These nonstripping angular distributions are not necessarily isotropic or symmetric; they may have well-defined maxima, but the complete angular distributions do not have the character of stripping curves. Examples are given in Fig. 3. Where contaminant groups obscure the proton peaks from a given state at the forward angles so that θ_{max} is uncertain, the column l_n is left blank.

IV. DWBA ANALYSIS OF THE (d,p) DATA

The angular distributions of protons from the (d,p) reaction were analyzed in terms of calculations with the computer code JULIE,[14] which uses the distorted-wave Born approximation (DWBA) and the zero-range approximation. In the particular calculations reported here, the spin-orbit interactions were neglected, no lower cutoffs were used in the radial integrals, surface absorption was assumed, and the neutron well was taken as being of the Woods-Saxon type.

For the deuteron and for the proton, the form of the optical well used in these calculations was

$$U(r) = -\frac{V}{1+e^x} + iW\frac{d}{dx'}\frac{1}{1+e^x} + V_c(r,r_c), \qquad (1)$$

where $x=(r-r_0A^{1/3})/a$; $x'=(r-r_0'A^{1/3})/a'$; and $r_c=r_{0c}A^{1/3}$. The parameters V and W are the depths of the real and imaginary potentials, respectively, and V_c is the Coulomb potential derived from a uniform charge density of radius r_c. The parameters for both particles have been found to be nonunique in giving good fits to

14 R. H. Bassel, R. M. Drisko, and G. R. Satchler, Oak Ridge National Laboratory Report, ORNL-3240, Office of Technical Services, Department of Commerce, Washington 25, D. C. (unpublished).
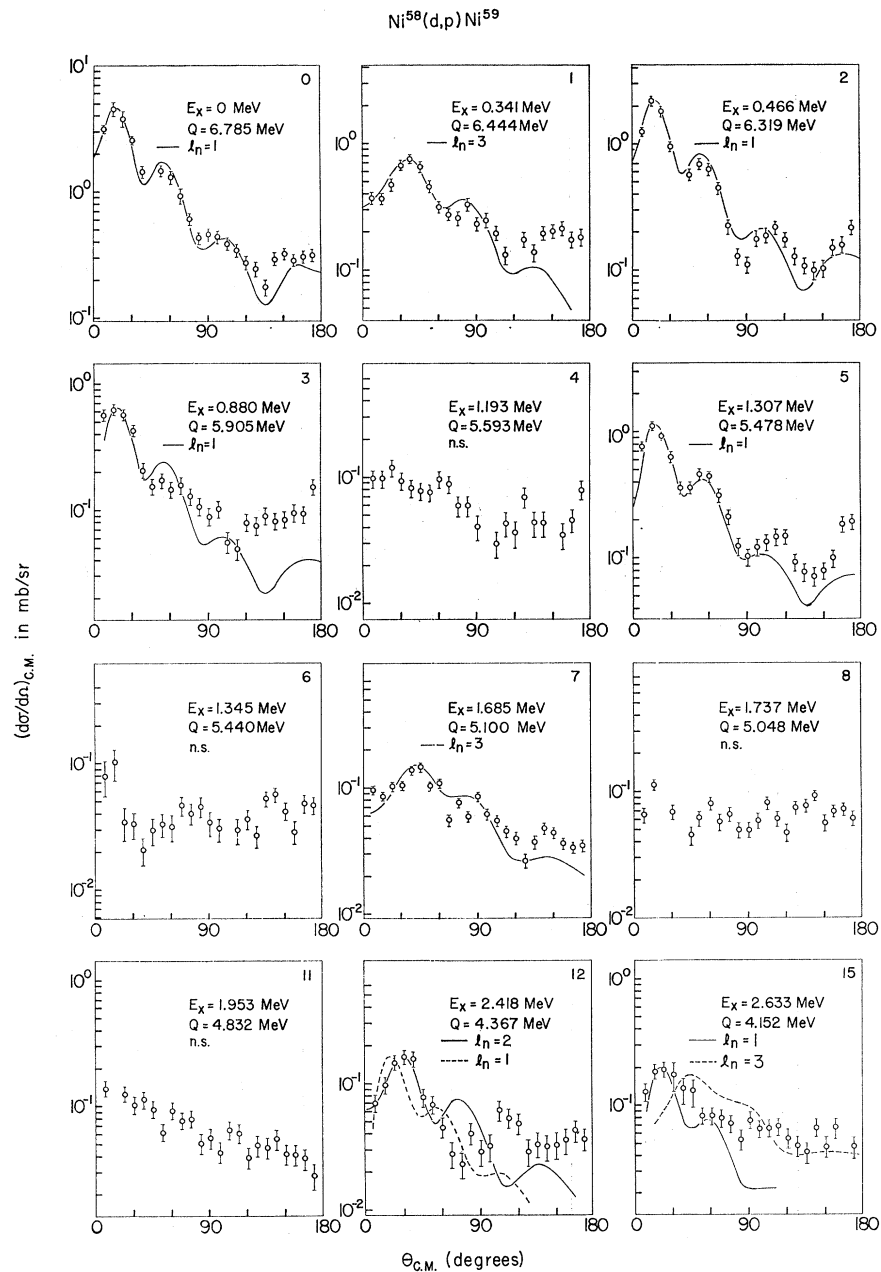
FIG. 3. Angular distributions of some proton groups from the $Ni^{58}(d,p)Ni^{59}$ reaction. At the top right of each drawing is the number used to identify the corresponding state in Table II. The circles represent the experimental data, and the vertical bars give the statistical error. The curves are derived from DWBA calculations assuming the indicated l_n and Q values.

elastic-scattering data.[15] The deuteron parameters affect the calculational results on the (d,p) angular distributions far more critically than those of the proton, and therefore greater care must be exercised in their choice. The proton parameters used here were extrapolated from fits to data obtained by Perey[16] and were $V=52$ MeV, $r_0=1.25$ F, $a=0.65$ F, $W=42$ MeV, $r_0'=1.25$ F, $a'=0.47$ F, and $r_{0c}=1.3$ F. Several sets of

deuteron parameters[17,18] that have previously given reasonable fits to (d,p) data from this mass region were tested in the case of two levels in Ni^{59} whose spins are known; namely, the ground state $(l_n=1, J^\pi=\frac{3}{2}^-)$ and the first excited state $(l_n=3, J^\pi=\frac{5}{2}^-)$. Table III shows these parameters, together with the spectroscopic factors $S(0)$ and $S(1)$ deduced from fitting the (d,p) data for these two transitions.

[15] R. H. Bassel, R. M. Drisko, G. R. Satchler, L. L. Lee, Jr., J. P. Schiffer, and B. Zeidman, Phys. Rev. **136**, B960 (1964); **136**, B971 (1964).
[16] F. G. Perey, Phys. Rev. **131**, 745 (1963).

[17] P. D. Barnes, C. K. Bockelman, Ole Hansen, and A. Sperduto, Phys. Rev. **135**, B438 (1964).
[18] T. A. Belote, H. Y. Chen, Ole Hansen, and J. Rapaport, this issue, Phys. Rev. **142**, 624 (1966).
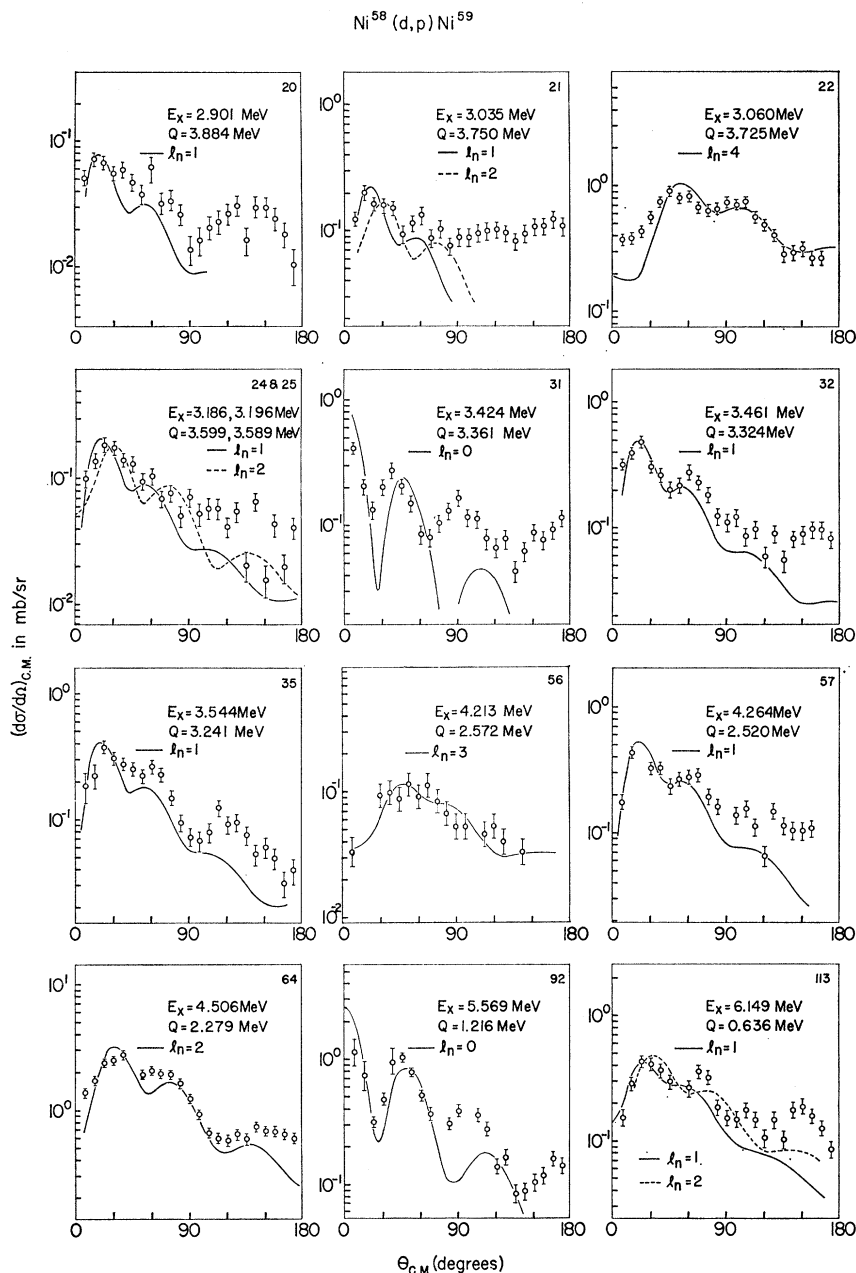
Ni⁵⁸ (d,p) Ni⁵⁹

FIG. 4. $Ni^{58}(d,p)Ni^{59}$ angular distributions (continued).

No data on elastic scattering of 7-MeV deuterons were taken in the course of this work. However, in connection with current work in this laboratory on other nickel isotopes, a complete angular distribution was obtained of the elastically scattered deuterons from Ni^{60} at 7.5 MeV. It was assumed that optical-model parameters resulting from a DWBA analysis of these data would not be significantly different from the parameters that might be obtained[19] for 7-MeV deuterons on Ni^{58}. Therefore, the sets labeled P and T in Table III were used as points of departure in attempts

to fit these elastic-scattering data from Ni^{60}. This was done with the automatic search program ABACUS.[20] The parameters V, W, a, and a' were varied, while r_0, r_0', and r_{0c} were kept fixed. The resulting sets of parameters are labeled PA and TA, respectively, and both sets produced equally good fits to the experimental $Ni^{60}(d,d)Ni^{60}$ angular distribution. The resultant fit for the potential TA is shown in Fig. 5. The circles are the data points, and the curve represents the calculated differential cross section.

[19] L. L. Lee, Jr., and J. P. Schiffer, Phys. Rev. 134, B765 (1964).

[20] E. H. Auerbach, Brookhaven National Laboratory Report BNL-6562 (ABACUS-2), 1962 (unpublished).

In Fig. 6, theoretical DWBA curves are compared with the experimental data points for the ground state $(l_n = 1)$ and for the first excited state $(l_n = 3)$ in the Ni⁵⁸(d,p)Ni⁵⁹ case. Since the spectroscopic results in Table III are all within the uncertainty claimed for the DWBA calculations, the choice of the parameters in the (d,p) calculations was made on the basis of an acceptable fit to the elastic-scattering data and of the best fit to the (d,p) data. Consequently, set TA was chosen to extract the strength functions $(2J+1)S_{l_n,j}$ throughout the energy region covered in the (d,p) reaction. Undoubtedly, other families of parameters could have been found that would have given equally good fits to the Ni⁶⁰(d,d) data; however, no extensive searches for such sets were carried out.
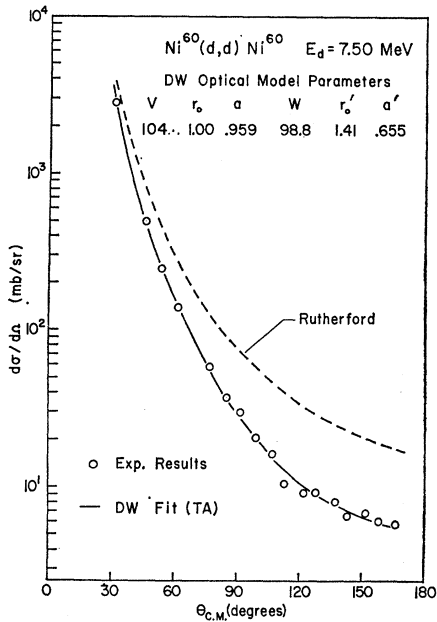
FIG. 5. The angular distribution of elastically scattered deuterons from Ni⁶⁰ at 7.50 MeV. The circles represent experimental data, and the solid curve is the DWBA prediction using the optical-model parameters shown in the figure (potential TA of Table III).

To obtain the values of the strength function $(2J+1)S_{l_n,j}$ for the stripping transitions, we have used the following relationship between the experimental cross section $d\sigma/d\Omega$ and the calculated reaction function $\sigma(l_n,Q,E_d,\theta)$:

$$d\sigma/d\Omega = 1.48 \frac{(2J_f+1)}{(2J_i+1)} S_{l_n,j} \sigma(l_n,Q,E_d,\theta). \quad (2)$$

Here, J_i and J_f are the angular momenta of the initial and final nuclear states, respectively, and j is the total angular momentum of the transferred neutron, restricted to the values $j = l_n \pm \frac{1}{2}$. In the present case, $J = 0$, and this gives $J_f = j$. Since J_f is not known for most of the levels, we cannot give the values of the

TABLE III. Deuteron parameters and resulting spectroscopic factors.

Set[a]	V	r_0	a	W	r_0'	a'	$\frac{S(0)}{2p_{3/2}}$	$\frac{S(1)}{1f_{5/2}}$	$S(1)/S(0)$
P	98	1.15	0.81	76.8	1.34	0.680	0.635	0.589	0.927
PA	92.4	1.15	0.789	76.8	1.34	0.685	0.542	0.518	0.955
T	103	1.00	0.900	100	1.41	0.650	0.71	0.71	1.00
TA	104.4	1.00	0.959	98.8	1.41	0.655	0.685	0.66	0.965
C1	112	1.00	0.900	76	1.55	0.470	0.617	0.479	0.777
C2	116.2	1.00	0.782	52.6	1.47	0.662	0.688	0.524	0.784

[a] Identification symbols for the sets: P = Perey (Ref. 16) parameters extrapolated to Ni⁵⁸; PA = parameters obtained from ABACUS search to fit Ni⁶⁰(d,d) data, starting with P; T = average of parameters found to fit the Ti isotopes best (Ref. 17); TA = parameters obtained from ABACUS search starting with T; C1 = average parameters found in fitting deuteron elastic-scattering data on the Ca isotopes at several bombarding energies (Ref. 15); C2 = parameters found to fit (d,p) and elastic-scattering data on Ca⁴⁶ at 7.0-MeV bombarding energy (Ref. 18).

spectroscopic factors $S_{l_n,j}$, only those for $(2J+1)S_{l_n,j}$. In the figure and tables, we drop the subscript f on J_f. The theoretical cross section $\sigma(l_n,Q_d,E,\theta)$ depends on the shape of the wave function of the captured neutron and, thus, on the depth of the neutron well, which was adjusted to give the correct separation energy for the last neutron in Ni⁵⁹ in the residual state considered. The resulting dependence of the calculated maximum cross section on Q is shown in Fig. 7 for $l_n = 1, 2,$ and 3. All the values of $(2J+1)S_{l_n,j}$ and of $S_{l_n,j}$ presented in the next
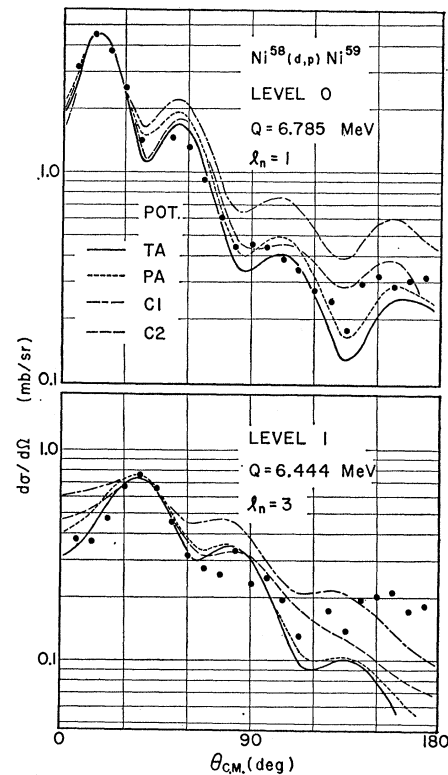
FIG. 6. Differential cross sections for the ground state $(l_n = 1)$ and the first excited state $(l_n = 3)$ from the Ni⁵⁸(d,p)Ni⁵⁹ reaction at 7.0 MeV. The points are the experimental data, and the curves are the DWBA predictions for various sets of optical potential parameters given in Table III.
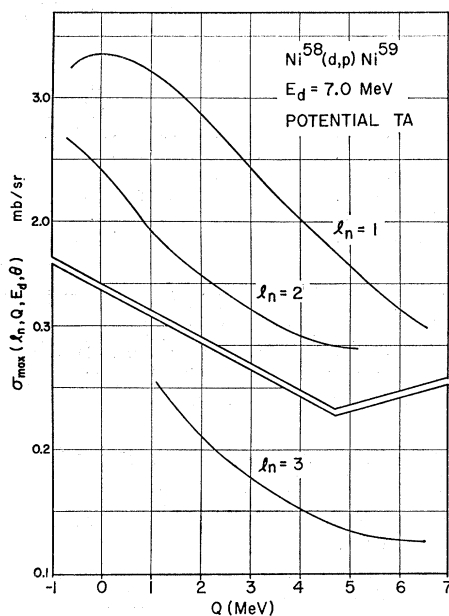
FIG. 7. Q and l_n dependence of $\sigma(l_n,Q,E_d,\theta)$ as calculated from DWBA theory using optical potential parameters labeled TA in Table III. The curves show the maximum value of σ as a function of Q for $l_n=1$, 2, and 3 and $E_d=7.0$ MeV.

section have been obtained from Eq. (2) by using the values of the cross sections corresponding to the maximum of the distribution.

Sherr et al.[21] have suggested another prescription for extracting spectroscopic factors that seems to be an improvement over the above method in some cases. Instead of varying the neutron well depth to produce the correct separation energy for each Ni^{59} state, one fixes a constant separation energy equal to the single-particle energy for each of the classes of states $j=l_n+\frac{1}{2}$ and $j=l_n-\frac{1}{2}$. The spectroscopic factor, $S_{l_n,j}$, for each state of a given j is then extracted by using the theoretical cross section $\sigma(l_n,Q,E_d,\theta)$ calculated for the corresponding constant separation energy. As further discussed in Sec. V.A, we have tried to apply this procedure to the $l_n=1$ and $l_n=3$ strengths of the present data. For the $2p_{3/2}$ and $2p_{1/2}$ strengths, these results are highly speculative, since only a few of the levels have known J values.

V. CONCLUSIONS AND COMPARISON WITH OTHER DATA

A. Level Scheme and Spectroscopic Factors

The increased resolution in these experiments has enabled many previously unresolved levels to be examined in more detail. Figure 8 shows the level schemes for Ni^{58} and Ni^{59}, and Fig. 9 shows the distribution of

[21] R. Sherr, Argonne National Laboratory Report No. ANL 6878, p. 207 (unpublished); and R. Sherr, E. Rost, and B. Bayman, Bull. Am. Phys. Soc. 8, 458 (1964).

spectroscopic strengths to each of the orbitals corresponding to $l_n=0$, 1, 2, 3, and 4 in Ni^{59} assigned from our analysis. The ordinates are proportional to $(2J+1)S_{l_n,j}$. The $l_n=1$ strength is highly fragmented over a span of 6.5 MeV, indicating strong residual interactions. Only three $l_n=3$ levels are seen, at 0.341, 1.685, and 4.213 MeV. The $l_n=0$ and $l_n=2$ transitions, presumably corresponding to $3s_{1/2}$ and $2d$ states, are also spread out in energy, and undoubtedly many such transitions occur at higher energies than could be reached in this experiment. All the $g_{9/2}$ strength appears to be concentrated in the one $l_n=4$ level at 3.060 MeV.

The shell-model sum rule[22] for (d,p) stripping is

$$\sum_a \frac{(2J_f+1)S_{l_n,j}{}^a}{(2J_i+1)}$$

$= $ number of (l_n,j) neutron holes in the target.   (3)

This sum is taken over all final states with a given set of n, l_n, and $j=J_f$. Line 1 of Table IV gives the sums of the experimentally deduced values of $(2J+1)S_{l_n,j}$ added from column 7 of Table II for the cases of the
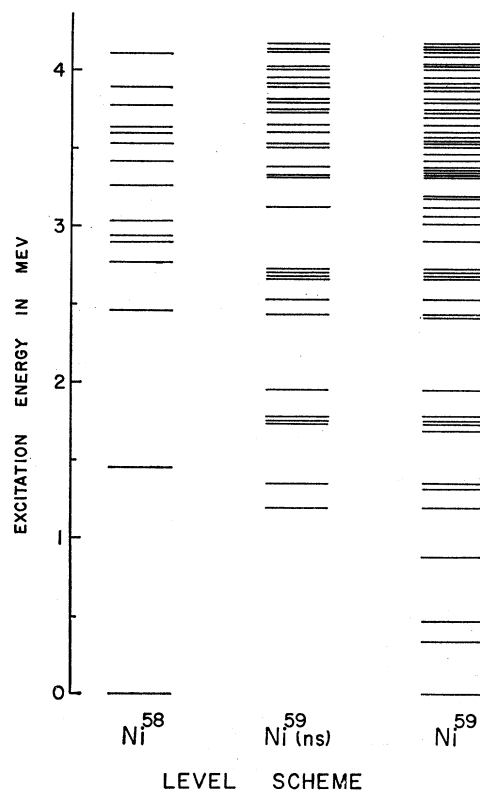
FIG. 8. The energy spectra of Ni^{58} and Ni^{59} below 4.1 MeV, as found from the (p,p') and (d,p) reactions on Ni^{58}. The center scheme shows only the nonstripping levels (n.s.) from the $Ni^{58}(d,p)Ni^{59}$ reaction, while the first and third columns include all the levels in Ni^{58} and Ni^{59} found in these experiments.

[22] M. H. Macfarlane and J. B. French, Rev. Mod. Phys. 32, 567 (1960); and S. Yoshida, Nucl. Phys. 38, 380 (1962).
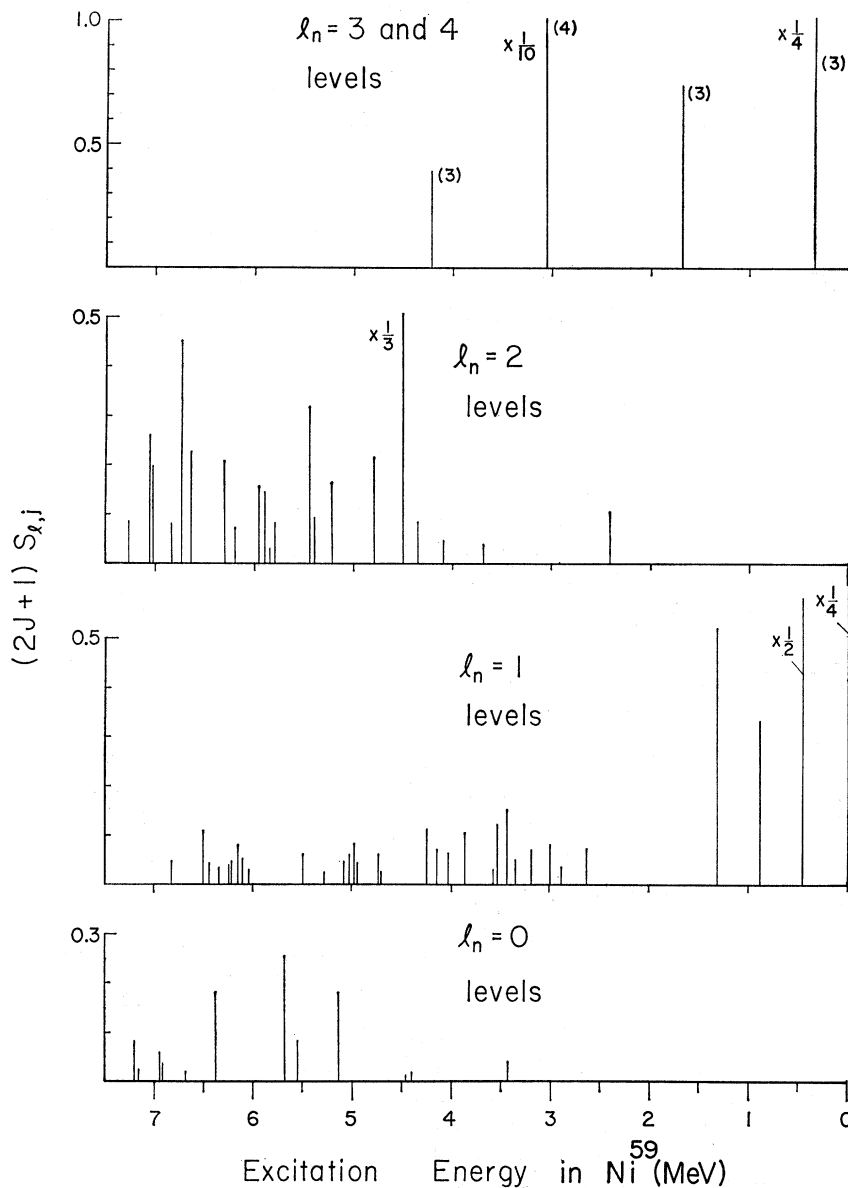
FIG. 9. The spectroscopic strengths $(2J+1)S_{l_n,j}$ listed in Table II are plotted as a function of excitation energy for the observed values of the orbital angular momentum of the transferred neutron l_n.

$l_n = 0$, 1, 2, 3, and 4 transitions. It is assumed here that these transitions populate only the $3s_{1/2}$, $2p$, $2d$, $1f_{5/2}$, and $1g_{9/2}$ states, respectively. As discussed in Sec. IV, these DWBA predictions are based on a neutron well depth adjusted to produce the actual neutron separation energy for each level in Ni^{59}. Lines 2 and 3 of Table IV give the pairing model[2] and simple shell-model predictions for the right-hand side of Eq. (3) in the case of each of the above orbitals. The predictions from pairing theory result from considerations based on configuration admixture of the simple shell-model states produced by the residual pairing interaction.

Because of the approximations made in the DWBA calculations, the spectroscopic factors obtained may be in error by 30% or more. Thus, only general indications

should be expected from the results quoted in Table IV. Accordingly, the $2p$ and $1f_{5/2}$ experimental sum strengths cannot be taken as an accurate measurement of the configuration admixture in the Ni^{58} ground state. The results actually are in agreement with theoretical predictions within the limits of error. Other factors, however, may also contribute to the excess $2p$ strength

TABLE IV. Sum-rule strengths $\Sigma_a(2J+1)S_{l_n,j}{}^a$.

	$2p$	$1f_{5/2}$	$1g_{9/2}$	$3s_{1/2}$	$2d$
Experiment	6.6	5.2	10.6	0.96	4.5
Pairing theory	4.6	5.4	9.9	2.0	10.0
Simple shell model	4.0	6.0	10.0	2.0	10.0

TABLE V. $Ni^{58}(d,p)Ni^{59}$ sum-rule analysis using the fixed-Q approach.

Case	Configuration	$\Sigma_a S_{l_n i}{}^a$ (c)	(d)	(e)	$E_{l,i}$ (MeV) (c)
(a)	$2p_{3/2}$	0.76	0.67	0.50	0.11
	$2p_{1/2}$	1.30	0.96	1.0	2.4
(b)	$2p_{3/2}$	0.77	0.67	0.50	1.3
	$2p_{1/2}$	1.18	0.96	1.0	3.4
	$1f_{5/2}$	0.88	0.90	1.0	1.0

Case (a) $J=\frac{3}{2}^-$ for levels No. 0 and 3. $J=\frac{1}{2}^-$ for remaining 31 $l_n=1$ levels.
Case (b) $J=\frac{3}{2}^-$ for levels No. 0, 3, 32, 35, 44, 58, and 79.
Case (c) From experimental DWBA analysis.
Case (d) Pairing theory.
Case (e) Simple shell model.

indicated in the table. For instance, some of the weak transitions assigned $l=1$ (in this work) may in fact be due to configurations other than $2p$ (see the discussion of level Nos. 15 and 21 in Sec. V-B). The $g_{9/2}$ strength seems to be carried completely by the one $l_n=4$ level observed, whereas the $3s_{1/2}$ and $2d$ level sum strengths indicate that many of these levels lie outside the energy range of this experiment.

The alternative constant Q-value prescription in the distorted-wave analysis mentioned in Sec. IV has been applied to the $l_n=1$ and $l_n=3$ states. In order to do this, it is necessary to assign spins to each of the levels involved. In the case of the $l_n=1$ distributions, only four of the 33 levels reported here (namely, Nos. 0, 2, 3, and 5) have known J^π assignments.[6,23] These are $\frac{3}{2}^-$, $\frac{1}{2}^-$, $\frac{3}{2}^-$, and $\frac{1}{2}^-$, respectively. In Fig. 3, one observes that the characteristic Lee-Schiffer back-angle behavior[24] in the angular distributions of these levels seems to support these assignments. At the bombarding energy used in this experiment, however, there are no clearly convincing dips to permit distinguishing between $J=\frac{1}{2}$ and $J=\frac{3}{2}$ from the $l_n=1$ distributions of higher excited states. Consequently, the sum-rule strengths were deduced from the constant Q-value approach by making reasonable assignments with the restriction of holding the $2p_{3/2}-2p_{1/2}$ spin-orbit splitting to approximately 2 MeV. In Table V, two cases are shown; in the first extreme case (a), levels Nos. 0 and 3 alone are $2p_{3/2}$, and the remaining 31 levels arbitrarily are assumed to be $2p_{1/2}$. In the second case (b), levels Nos. 0, 3, 32, 35, 44, 58, and 79 are assigned spin $\frac{3}{2}^-$, and the remaining 26 levels are assigned spin $\frac{1}{2}^-$.

The spectroscopic factors $(S_{l_n,i})$ and single-particle energies $(E_{l,i})$ thus deduced are reasonable in both cases, particularly in view of the relatively large uncertainties in the spin assignments, the DWBA analysis, and the nuclear-model predictions.

The three levels, Nos. 1, 7, and 56, assigned $l_n=3$ distributions are all assumed to belong to the $1f_{5/2}$ orbital. The resulting spectroscopic factors show little change from those deduced by the previous treatment with a variable separation energy (Table IV).

Many angular distributions of a nonstripping character were observed in this experiment. They are associated with states in Ni^{59} that cannot be formed simply by coupling a single neutron to $Ni^{58}(0)$; hence, they must be populated by higher order reaction processes. For example, they may arise from compound-nucleus formation or from core excitation, where the excitation of the core is of single-particle or of phonon character. Figure 8 gives a comparison of the low-lying nonstripping (n.s.) levels in Ni^{59} with the Ni^{58} spectrum. Some clustering of nonstripping states is noted at the energy of the first 2^+ state in Ni^{58}, which might be expected from weak coupling of a particle to the 2^+ phonon. The density of the nonstripping levels is also high, at an energy of about 2.5 MeV, which is approximately equal to the energy gap in Ni^{58}. The angular distributions for these nonstripping levels in this experiment seem to show no systematic characteristics. However, from recent observations[25] in this laboratory on the study of detail structure in the angular distributions of nonstripping states, there are indications that improved statistics may yet shed more light on these levels via the (d,p) reaction. Further comment on some of these levels will be made in the following section.

B. Comparison with Other Data and Discussion of Results

The $Ni^{58}(d,p)Ni^{59}$ reaction has been studied by Fulmer et al.[4] with 12-MeV incident energy, and their results are given in columns 8, 9, and 10 of Table II for comparison with the present analysis. They resolve 89 levels in Ni^{59} up to 7.54 MeV, compared with 173 levels identified from our measurements in the same excitation region. From 7.54 to 9.3 MeV, Fulmer et al.[4] have identified an additional 46 levels in Ni^{59}. Their l_n assignments are in agreement with ours in the cases of the more prominent "stripping" levels, but are in disagreement with a number of the weaker groups. Specific comments on the angular-distribution assignments follow.

The $l_n=4$ Distributions

In Ref. 4, four levels are given $l_n=4$ assignments, only one of which agrees with our results. In the remaining three levels, we have given three different assignments, as follows:

$l_n=(0)$ to No. 63 at 4.470 MeV,

$l_n=(1)$ to No. 69 at 4.709 MeV,

n.s. to No. 88 at 5.429 MeV.

[23] R. E. Cote, H. E. Jackson, L. L. Lee, Jr., and J. P. Schiffer, Phys. Rev. 135, B52 (1964); and K. H. Fulmer and W. W. Daehnick Argonne National Laboratory Report No. ANL 6878, p. 303 (unpublished).
[24] L. L. Lee, Jr., and J. P. Schiffer, Phys. Rev. Letters 12, 108 (1964); and Phys. Rev. 136, B405 (1964).

[25] T. A. Belote, W. E. Dorenbusch, Ole Hansen, and J. Rapaport, Nucl. Phys. 73, 321 (1965).

Our only $l_n = 4$ assignment (No. 22 at 3.060 MeV) appears to fulfill completely the sum-rule prediction of $S=1$ for the spectroscopic factor (assuming the $1g_{9/2}$ state). Our value of the unperturbed single-particle energy, $E'_{9/2}$, for the $1g_{9/2}$ state is therefore 3.06 MeV, compared with 3.5 MeV from Ref. 4.

The $l_n = 3$ Distributions

Two prominent $l_n = 3$ distributions (Nos. 1 and 7) are observed in both (d,p) experiments. In addition, in Ref. 4, level No. 15 was also assigned $l_n = 3$, and in the present work, level No. 56 was given a probable $l_n = (3)$ assignment. From recent observations discussed below, there is strong indication that only level Nos. 1 and 7 arise from neutron stripping to the $1f_{5/2}$ orbital. With this assumption, the present data give: $S=0.80$ and $E'_{5/2}=0.58$ MeV, compared with $S=0.88$ and $E'_{5/2}=0.94$ MeV if level No. 56 is included, and compared with $S=1.0$ and $E'_{5/2}=0.60$ MeV from Ref. 4, where level No. 15 was assumed to be a $1f_{5/2}$ state. The low value $E'_{5/2}$ for the $1f_{5/2}$ state is consistent with the trend[26] observed in $_{24}Cr_{31}^{55}$ and $_{26}Fe_{31}^{57}$, which indicates that, as the proton number is increased for a fixed neutron number $(N=31)$, the $1f_{5/2}$ single-particle energy decreases relative to the energies of the $2p$ states.

The $l_n = 2$ Distributions

Fulmer et al.[4] report 73 $l_n = 2$ distributions up to 9.3-MeV excitation, of which 30 are below 7.24 MeV, which is the limit of the angular-distribution analysis in the present experiment. Within this region, our data suggest instead 22 levels with $l_n = 2$ distributions, 16 of which are in agreement. Of the remaining six, Fulmer et al.[4] give an $l_n = (1)$ assignment to No. 12, $l_n = (0)$ to No. 51, and no assignment to 4 of these (Nos. 102, 107, 115, and 136). Fourteen of the 30 distributions assigned $l_n = 2$ in Ref. 4 are here given different assignments; namely, 8 to $l_n = 1$, one to $l_n = 3$, four to "n.s.," and no assignment to one (see Table II).

It is assumed that all $l_n = 2$ levels belong to the $2d$ orbitals. Since no distinction is possible between $2d_{5/2}$ and $2d_{3/2}$, we can only compare our value of 4.5 for the total $2d$ transition strength; i.e., $\sum (2J+1)S$, totaled over the 22 $l_n = 2$ states, with the value 4.6 from Ref. 4 totaled over the 30 levels within this same region of excitation. That the $2d$ states are highly fragmented and only partially excited within the excitation ranges covered in both experiments is evident from these figures (see Table IV and Fig. 9).

The $l_n = 1$ Distributions

Reference 4 reports 25 $l_n = 1$ distributions with none above 6.15 MeV. In the present work we have assigned $l_n = 1$ to 26 levels in the same excitation region, with

only four of these in disagreement. In addition, we have assigned $l_n = 1$ to six levels above 6.15 MeV. From both experiments, it appears that the total $2p$ strength (see Tables II and IV) is greater than expected. The possibility of incorrect assignments for both $l_n = 1$ and $l_n = 2$ is discussed below.

The $l_n = 0$ Distributions

In the case of seven levels in Ni⁵⁹, our assignments of $l_n = 0$ are in agreement with those of Ref. 4. Two (Nos. 51 and 63) are in disagreement. In the excitation region up to 7.24 MeV, there are an additional four levels from our analysis indicating $l_n = 0$, and in these cases no assignments were made in Ref. 4. The latter further makes one $l_n = 0$ assignment to one level (No. 130), for which our data were not complete.

All these $l_n = 0$ levels presumably correspond to stripping into the $3s_{1/2}$ state. The sum-rule analysis from both experiments indicates that about 50% of the $3s_{1/2}$ strength is observed below 7.24 MeV.

Stripping to Hole States and/or Higher Order Processes

Single-neutron pickup reactions on Ni⁶⁰ targets indicate $l_n = 3$ transitions leading to levels in Ni⁵⁹ at about 1.9, 2.6, 3.0, 4.17, and 7.28 MeV which appear to be of $f_{7/2}$ character. The most recent (p,d) and (d,t) results on these states are shown in Table VI, along with the results from our (d,p) analysis.

Level No. 11, designated "n.s.," does not have a typical stripping pattern (Fig. 3), and thus no DWBA calculation was attempted. An unbiased conventional assignment for Nos. 15 and 21 would be $l_n = (1)$; however, the $l_n = 1$ DWBA fit (Fig. 3) is admittedly not good when compared with other lower energy p-state distributions. On the other hand, the angle at which the maximum cross section is observed in these cases is not consistent with other $l_n = 3$ distributions corresponding to $f_{5/2}$ single-particle states (Nos. 1 and 7). In view of the J^π assignments from the pickup data in Table VI, it appears that the conventional criterion for assignment of the orbital angular momentum l_n from our (d,p) angular distributions is wrong, certainly

TABLE VI. Comparison of (p,d), (d,t), and (d,p) data.

Level No.	Ni⁵⁹(d,p)Ni⁶⁰[a]		Ni⁶⁰(p,d)Ni⁵⁹[b]		Ni⁶⁰(d,t)Ni⁵⁹[c]	
	E_x	l_n	E_x	J^π	E_x	J^π
11	1.953	n.s.	1.96	$\frac{1}{2}^-$	1.98	
15	2.633	(1)	2.63	$\frac{7}{2}^-$	2.65	$\frac{7}{2}^-$
21	3.035	(1)	3.04	$\frac{7}{2}^-$	3.09	$(\frac{7}{2}^-)$
56	4.213	(3)	4.17	$(\frac{7}{2}^-)$		
161	7.282	(d)	7.28	$\frac{7}{2}^-$		

a Present experiment.
b R. Sherr, B. F. Bayman, E. Rost, M. E. Rickey, and C. G. Hoot, Phys. Rev. 139, B1272 (1965).
c R. H. Fulmer and W. W. Daehnick, Phys. Rev. 139, B579 (1965).
d Data incomplete at forward angles.

26 C. A. Wiedner, A. Sperduto, H. A. Enge, and W. W. Buechner, Bull. Am. Phys. Soc. 10, 512 (1965).

in the cases of Nos. 15 and 21. The $l_n = (3)$ assignment to No. 56 does not rule out a possible ambiguity. Insufficient data at forward angles for level No. 161 have prevented an adequate interpretation of that angular distribution.

Two possible explanations for the anomalous behavior of our (d,p) distributions with regard to the reaction mechanism may be suggested for the above cases: (1) In view of the absence of any (d,p) transitions with typical $l_n = 3$ distributions at the energies of states Nos. 11, 15, and 21 in the present data, one conclusion may be that they correspond to $f_{7/2}$ core-excited states in Ni^{59} that cannot be reached by stripping. Thus, they may be populated by higher order (d,p) processes[27] resulting in irregular angular distributions. (2) An alternative explanation for these anomalous transitions is that they correspond to $f_{7/2}$ hole-state stripping; that is, (d,p) stripping to $f_{7/2}$ holes present in the $Ni^{58}(0)$ target. This would imply that such $l_n = 3$ neutron transfers display anomalous angular distributions at this bombarding energy. This alternative is consistent with the suggestion of incomplete closure in the $f_{7/2}$ shell made by Bassani et $al.$[7] from $Ni^{58}(p,t)Ni^{56}$ studies and by Fulmer and Daehnick[8] using the $Ni^{60}(d,t)Ni^{59}$ reaction. If indeed these levels correspond to $f_{7/2}$ hole transitions, the specific character of their stripping distributions may be used to extract more nearly accurate spectroscopic information than presently attainable via pickup transitions, particularly if better statistics are realized in the (d,p) data and refinements are made in the DWBA calculations. The differences observed here in the (d,p) angular distributions between $f_{5/2}$ stripping to single-particle states and (presumably) to $f_{7/2}$ hole excitations leading to states in the same residual nucleus are much more marked than the dif-

ferences reported in the angular distributions for levels corresponding to $f_{5/2}$ and $f_{7/2}$ states from pickup data.[6]

Evidence for such characteristic (d,p) angular distributions corresponding to stripping to $1d_{3/2}$ hole states in Ca^{41} and Ca^{43} and in Ti^{47} has already been observed in this laboratory.[28] More detailed analyses with improved data of (d,p) stripping to possible $f_{7/2}$ hole states are presently being carried out in the case of the $N = 29$ nuclei.

Some of the discrepancies, particularly in the instance of the $l_n = 2$ distributions discussed above, between the results of the (d,p) data of Fulmer et $al.$[4] obtained with 12-MeV incident deuterons and those from the present experiment at a bombarding energy of 7.0 MeV may of course be due to effects arising from incident energy dependence. However, the examples of the levels in Table VI do show the possibility of misinterpretation and point to the importance of good resolution and the need for better data.

ACKNOWLEDGMENTS

[27] S. K. Penny and G. R. Satchler, Nucl. Phys. **53**, 145 (1964).

[28] T. A. Belote, A. Sperduto, and W. W. Buechner, Phys. Rev. **139**, B80 (1965); W. E. Dorenbusch, T. A. Belote, and Ole Hansen (to be published); J. Rapaport, A. Sperduto, and W. W. Buechner, Phys. Rev. (to be published).